Atomic Force Microscopy Force Mapping in the Study of Supported Lipid Bilayers

ARTICLE *in* LANGMUIR · FEBRUARY 2011

Impact Factor: 4.46 · DOI: 10.1021/la103927a · Source: PubMed

3 AUTHORS:

James K Li
University of Toronto
18 PUBLICATIONS **194** CITATIONS
SEE PROFILE

Ruby May Arana Sullan
Max Planck Institute of Colloids and Interfaces
22 PUBLICATIONS **593** CITATIONS
SEE PROFILE

Shan Zou
National Research Council Canada
59 PUBLICATIONS **1,338** CITATIONS
SEE PROFILE

Langmuir
Article
pubs.acs.org/Langmuir

Atomic Force Microscopy Force Mapping in the Study of Supported Lipid Bilayers†

James K. Li,[§] Ruby May A. Sullan,[‡,§] and Shan Zou*,[‡]

[‡]*Steacie Institute for Molecular Sciences, National Research Council Canada, Ottawa, 100 Sussex Drive, Ottawa, ON K1A 0R6, Canada, and* [§]*Department of Chemistry, University of Toronto, 80 St. George Street, Toronto, ON M5S 3H6, Canada*

Received September 30, 2010. Revised Manuscript Received November 10, 2010

Investigating the structural and mechanical properties of lipid bilayer membrane systems is vital in elucidating their biological function. One route to directly correlate the morphology of phase-segregated membranes with their indentation and rupture mechanics is the collection of atomic force microscopy (AFM) force maps. These force maps, while containing rich mechanical information, require lengthy processing time due to the large number of force curves needed to attain a high spatial resolution. A force curve analysis toolset was created to perform data extraction, calculation and reporting specifically in studying lipid membrane morphology and mechanical stability. The procedure was automated to allow for high-throughput processing of force maps with greatly reduced processing time. The resulting program was successfully used in systematically analyzing a number of supported lipid membrane systems in the investigation of their structure and nanomechanics.

Introduction

Since its introduction nearly 25 years ago, the atomic force microscope (AFM) has been extensively used in a large number of systems to investigate interactions at submicrometer length scales and forces in the pico- to nano-Newton regime.[1−6] In AFM imaging, a tip at the end of a cantilever is raster-scanned across an area of interest, and the cantilever's deflection for example, is used as feedback to adjust the height of the cantilever base relative to the sample surface. In this way, heterogeneities on the sample can be distinguished via relative differences in the actual heights of the region's domains or from chemical differences that still effectively cause the cantilever base to adjust its height.

AFM force spectroscopy[7] offers a more rigorous and quantitative approach by inducing a tip−sample interaction event and recording the same channels of data over a period of time. In addition, the induced tip−sample interaction is done without lateral movement of the sample relative to the cantilever, so the interpretation of the response is simplified. The data that is collected over time can be analyzed for kinetics and mechanics, for example, and with repetition statistics.

By extension, AFM force mapping—the collection of an array of force curves with record of each one's spatial position—would be able to elucidate the spatial dependence of the interaction forces. The collection and analysis of force maps can be logically organized in the flowchart shown in Scheme 1. While there have been some mechanical investigations via AFM force maps in the literature, it is not as commonplace (especially at high resolutions) because of the inherent difficulties in maintaining stability during the lengthy data collection stage and in the subsequent analysis of a very large amount of force curves, which are both necessary in obtaining sufficiently spatially dense data to have high resolution.[8]

The issue of data collection is largely resolved due to stable setups and increased functionality in current instrumentation as well as automated force curve-collection over the region of interest. Force maps of greater than 64×64 pixels performed over a $3 \times 3\ \mu$m area with spatial resolution of ~50 nm is readily achievable and typically takes half an hour to collect. The challenge is in the extraction or calculation of several parameters during analysis of the thousands of force curves for each force map. As mentioned, while data collection is already automated by sophisticated software packaged with the instrument, batched data analysis is not provided. One large barrier to automation is the wide range and specificity of end-user needs, which makes the creation of a universally applicable program very difficult. The aim of this work, therefore, is to create a tool for the automated, batched analysis of force curves.

The system that we chose to investigate is that of supported lipid bilayers. The study of lipid bilayer membranes is a very active area of research in the biophysical sciences due to the ubiquity and importance of these types of platforms in a host of cellular functions.[9−11] For example, membranes enriched with cholesterol and sphingolipids have been implicated in protein binding, signal transduction, and programmed cell death.[12,13] The AFM imaging mode has been used with much success for these systems, due to its

† Part of the Supramolecular Chemistry at Interfaces special issue.

*To whom correspondence should be addressed. Address: Biomolecular Sensing and Imaging Group, Steacie Institute for Molecular Sciences, National Research Council Canada, 100 Sussex Drive, Rm 1095, Ottawa, ON K1A 0R6, Canada. Phone: 613 949-9675. Fax: 613 991-4278. E-mail: Shan.Zou@nrc-cnrc.gc.ca.

(1) Binnig, G.; Quate, C. F.; Gerber, C. *Phys. Rev. Lett.* **1986**, *56*, 930.
(2) El Kirat, K.; Morandat, S.; Dufrene, Y. F. *Biochim. Biophys. Acta, Biomembr.* **2010**, *1798*, 750.
(3) Engel, A.; Muller, D. J. *Nat. Struct. Biol.* **2000**, *7*, 715.
(4) Garcia-Manyes, S.; Sanz, F. *Biochim. Biophys. Acta, Biomembr.* **2010**, *1798*, 741.
(5) Goksu, E. I.; Vanegas, J. M.; Blanchette, C. D.; Lin, W. C.; Longo, M. L. *Biochim. Biophys. Acta, Biomembr.* **2009**, *1788*, 254.
(6) Muller, D. J.; Krieg, M.; Alsteens, D.; Dufrene, Y. F. *Curr. Opin. Biotechnol.* **2009**, *20*, 4.
(7) Cappella, B.; Dietler, G. *Surf. Sci. Rep.* **1999**, *34*, 1.
(8) Seantier, B.; Giocondi, M. C.; Le Grimellec, C.; Milhiet, P. E. *Curr. Opin. Colloid Interface Sci.* **2008**, *13*, 326.
(9) Yeagle, P. *The Structure of Biological Membranes*; CRC Press: Boca Raton, FL, 2005.
(10) Brown, D. A.; London, E. *Annu. Rev. Cell Dev. Biol.* **1998**, *14*, 111.
(11) Siskind, L. J.; Colombini, M. *J. Biol. Chem.* **2000**, *275*, 38640.
(12) Bollinger, C. R.; Teichgraber, V.; Gulbins, E. *Biochim. Biophys. Acta, Mol. Cell Res.* **2005**, *1746*, 284.
(13) Simons, K.; Ikonen, E. *Nature* **1997**, *387*, 569.

Scheme 1. Flowchart of Force Map Collection, Subsequent Analysis, and Data Output

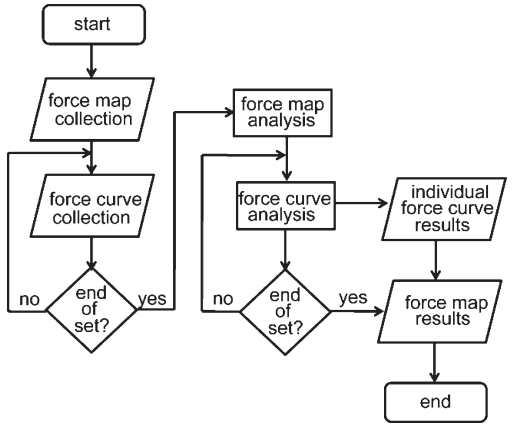

ability to visualize and probe at nanometer length scales.[14] However, as studies evolve from model lipid membranes to more biologically relevant, multicomponent mimics, the AFM's capabilities in distinguishing among heterogeneous microdomains in these systems may not be sufficient, and hence "imaging" by the generation of force maps provides a more rich and accurate picture.[15−20] While there has been earlier work on batched data analysis,[21−23] in this particular investigation, we establish a comprehensive package composed of an automation process to extract mechanical properties of lipid membranes undergoing AFM-tip indentation with the occurrence of membrane rupture. The universality of the tool is also demonstrated by its adaptation to process data from three different brands of commercial AFMs, as well as the ability to utilize several different mechanical models for the analysis of lipid membranes.

Methods

Materials. All lipids [1,2-dioleoyl-*sn*-glycero-3-phosphocholine (DOPC, 18:1), *N*-stearoyl-D-erythro-sphingosylphosphorylcholine (ESM, 18:0), and ovine wool cholesterol (Chol)] were purchased from Avanti Polar Lipids (Alabaster, AL) and used as received. HPLC-grade chloroform (ACP Chemicals Inc., Montreal, QC), ACS-grade methanol from Fisher Scientific (Ottawa, ON), and Milli-Q water, deionized to a resistivity of 18 MΩ·cm, were used in all of the experiments.

Lipid Bilayer Preparation. The preparation of lipid membranes supported on mica substrates utilized vesicle fusion protocols and is described in greater detail elsewhere.[18] In brief, lipid mixtures were obtained by combining the appropriate molar ratios of the different lipid components using chloroform and methanol as solvents: DOPC/ESM/Chol in a 2:2:1 molar ratio, referred to as DEC. The resulting solution was then exposed to a gentle stream of nitrogen and placed under vacuum overnight to further remove the solvents. The lipid film was hydrated to a final lipid concentration of 0.5 mg/mL for the DEC prior to use. Small unilamellar vesicles were obtained by sonicating the lipid solution to clarity (∼ 20−30 min) using a bath sonicator (Cole Parmer, Montreal, QC).

Scheme 2. Schematic of AFM Tip-Supported Lipid Bilayer Interaction: (a) Noncontact; (b) Tip−Bilayer Contact; (c) Bilayer Indentation; (d) Bilayer Rupture (Tip Breakthrough); (e) Tip−Substrate Contact

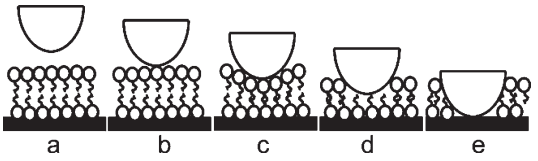

AFM Imaging and Force Mapping. AFM experiments were performed primarily using the Nanowizard II BioAFM (JPK Instruments, Berlin, Germany) mounted on an Olympus 1 × 81 inverted confocal microscope, operating in contact mode. The Asylum MFP-3D (Asylum Research, Santa Barbara, CA) and the Picoforce Scanning Probe Microscope (Veeco, CA) were also utilized. Silicon nitride cantilevers (DNP-S, Veeco, CA) were used in contact mode imaging and force mapping measurements unless stated otherwise. The spring constant, which was typically in the range of 0.15−0.28 N/m, was determined by the thermal noise method.[24] In force mapping, arrays of force distance curves were collected on bilayer samples with selected grid sizes (e.g., 64 × 64 pixels), and the two-dimensional (2D) visual maps were reconstructed using the custom analysis code described below. Applied loads within the range of 4−25 nN were typically used.

Results and Discussion

AFM-Tip Indentation with Membrane Breakthrough. The schematic for an AFM tip approaching, indenting, breaking through, and finally withdrawing from a supported lipid bilayer is shown in Scheme 2. When the approaching tip is still sufficiently far from the surface (the noncontact region), interaction forces are negligible (a) until the tip contacts the surface (b). As the approach is continued, an increasing, nonzero force is observed, and, since the sample is softer than the tip, the sample is indented (c). When the lipid can no longer sustain these loading forces, the tip breaks through the lipid (d), until it reaches the substrate (e). If tip approach continues beyond this point, the cantilever starts to deflect as the hard substrate cannot be indented.

The aforementioned set of events makes up the approach portion of the force curve. The tip is then withdrawn from the surface, and the remaining event it experiences is some adhesion to the sample before the tip pulls away and is again not in contact.

Observables and Calculations. From the approach and retract force curves, several useful parameters can be extracted: breakthrough forces, bilayer thickness (or penetration depth), Young's modulus values, and adhesion forces (Figure 1).

Breakthrough force is the magnitude of the force at which the lipid membranes finally rupture (relative to the "zero" force felt when very far away from contact). Indentation until rupture reveals the location of the substrate, and therefore allows the membrane thickness to be ascertained; it is the distance from the contact point to the substrate (Figure 1A−C).

Adhesion force can be calculated by taking the magnitude of the force from the retract data just prior to pull-off of the AFM tip from the surface (Figure 1D,E).

The elastic modulus is a mechanical property of the lipid layer that can be obtained by fitting the indentation region of the approach curve (Figure 1A,B) to an appropriate mechanical model for tip−sample interaction. Several models were utilized, and their

(14) Johnston, L. J. *Langmuir* **2007**, *23*, 5886.
(15) Dufrene, Y. F.; Barger, W. R.; Green, J. B. D.; Lee, G. U. *Langmuir* **1997**, *13*, 4779.
(16) Sullan, R. M. A.; Li, J. K.; Hao, C. C.; Walker, G. C.; Zou, S. *Biophys. J.* **2010**, *99*, 507.
(17) Sullan, R. M. A.; Li, J. K.; Zou, S. *Langmuir* **2009**, *25*, 12874.
(18) Sullan, R. M. A.; Li, J. K.; Zou, S. *Langmuir* **2009**, *25*, 7471.
(19) Canale, C.; Jacono, M.; Diaspro, A.; Dante, S. *Microsc. Res. Tech.* **2010**, *73*, 965.
(20) Ip, S.; Li, J. K.; Walker, G. C. *Langmuir* **2010**, *26*, 11060.
(21) Lin, D. C.; Dimitriadis, E. K.; Horkay, F. *J. Biomech. Eng.* **2007**, *129*, 430.
(22) Sugisaki, K.; Nakagiri, N. *Appl. Surf. Sci.* **1999**, *144−45*, 613.
(23) Sugisaki, K.; Nakano, K.; Sugimura, H.; Kandaka, N.; Nakagiri, N. *Jpn. J. Appl. Phys.* **1998**, *37*, 3820.
(24) Hutter, J. L.; Bechhoefer, J. *Rev. Sci. Instrum.* **1993**, *64*, 1868.

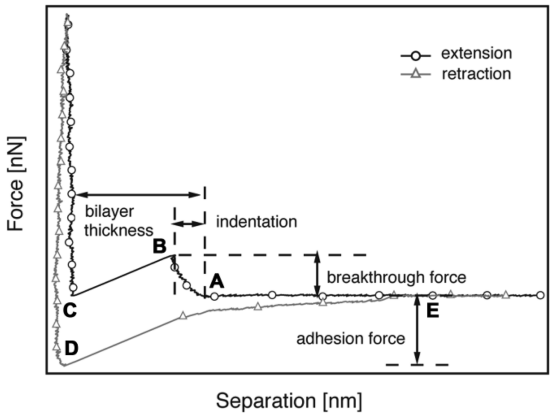

Figure 1. Force curves indicating quantities extracted: breakthrough force, indentation region, and adhesion force. Points of interest: A, contact point; B, onset of rupture/breakthrough; C, onset of substrate; D, maximum adhesion; E, sufficiently far from the surface with negligible adhesion effects.

suitability was evaluated on the basis of fit errors and comparison of calculated Young's modulus to literature data. The most appropriate model to describe the mechanics of this system was that of Sneddon's, which considers a semi-infinite sample contacted by a paraboloidal-shaped tip:

$$F = \frac{4E\sqrt{R}}{3(1-\sigma^2)}\delta^{3/2} \quad (1)$$

where E is Young's modulus, σ is Poisson's ratio, R is the tip radius, and δ is the indentation (separation distance rezeroed at the contact point).[25] The above equation can also be modified for conical-shaped tip geometry in the equation when sharper AFM tips are used in our experiments:

$$F = \frac{2E\tan(\alpha)}{\pi(1-\sigma^2)}\delta^2 \quad (2)$$

where α is the tip's semivertical angle.

These parameters arise from, or are affected by, specific and nonspecific tip−sample interactions. And, although there is some interdependence (e.g., breakthrough force and modulus values are calculated from the same region of the approach curve), when combined, they provide a more complete physical description of the system.

Batch Analysis of the Force Curves. The sets of force curves, ranging from approximately 1000 to 8000 curves, comprising the force map, were batch analyzed using a self-developed algorithm implemented in IGOR Pro 6 (Wavemetrics, Portland, OR). For each curve breakthrough force, Young's modulus, bilayer thickness, and adhesion force were calculated.

The program flow is depicted in Scheme 3. In the initial loading step (Scheme 3a), the set of force curves comprising the force map are read into the computer sequentially. This portion of the code was adapted to be able to process raw force map data from the three commercial instruments utilized. In addition to deflection force (F) versus distance (z) data, the spring constant k, and (x,y) position of each are recorded. The extension and retraction portion of the curves are separated. From the spring constant and using Hooke's Law, deflection distance d can be calculated by

$$d = \frac{F}{k} \quad (3)$$

and the tip−sample separation s can be calculated by

$$s = z - \frac{d}{c} \quad (4)$$

where c is a correction factor that is related to instrument sensitivity, and can be obtained via calibration, and fine-tuned at a later stage to counter the effects of minor drift.

Each force curve is then analyzed, and an internal parameter is calculated so that the subsequent analysis would be data-set-specific. The force curves are box smoothed, using a box size that would be appropriate for the desired distance resolution. The force curve $F(z)$ is then differentiated to obtain $F'(z)$. The differentiated curve will show a sharp peak in the regions when the force−distance curve indicates a breakthrough event (Scheme 3a). The standard deviation of $F'(z)$ is calculated for the region where the tip is in the noncontact region. The magnitude of this peak is compared to the standard deviation of the baseline region to calculate a standard-deviation multiple. This value will be used for threshold-detection of breakthrough events by calculating the average for the entire batch of force curves, and adjusting this average to accept more or less curves. This addresses data-set-specific tuning.

In the next step (Scheme 3b), this data set-averaged value is used as a threshold in searching for the $F'(z)$ peak again in each force curve. In this second pass, if the breakthrough peak of the specific force curve does not meet the threshold, it can be dropped from further analysis. Once the peak is found in $F'(z)$, three important reference points in $F(z)$ (the contact point and the two points indicating the onset and end of rupture (i.e., the substrate)) can be determined. Local maxima and minima searches in $F(z)$ in this region can be initiated to look for the latter two points.

For the contact point, a search algorithm was implemented to facilitate the batch analysis process. The algorithm assumes that the breakthrough point has already been found, and searches points only prior to it. To speed up the analysis, only a portion of the curve was searched, restricted to a predefined distance from the breakthrough point. Each point in the selected portion is evaluated as a candidate contact point with the following algorithm: the candidate point is the junction of a piece-wise function; any points before the candidate contact point are considered the noncontact region, and are fit to a straight line; points beyond this point up to the breakthrough point belong to the indentation region and are also fit to an appropriate function. Although a 3/2 power fit in this region may have been more accurate,[25] use of a second linear fit is much quicker, and given the evaluation scheme to be described, was not deemed necessary. The average mean square error of the proposed piecewise function and the experimental data is calculated, and the candidate point that provided the lowest mean square error becomes the contact point to be used for subsequent calculations. To further prevent false identification, an added criterion to ensure the candidate point is sufficiently close in force value to the noncontact region was implemented.

Data that are physically improbable (e.g., negative forces and negative separation distances) are filtered out and earmarked for manual inspection.

Data Analysis and Visualization. Data extracted from each force map can be presented in a number of ways as seen in Scheme 3c and explained below.

The collection of data from a force map provides two types of information: spatially correlated values and statistics. In order to visualize the former, two types of spatial maps were generated—contour plots and image plots—utilizing the (x,y) position recorded for each force curve. Images of breakthrough force, indentation, and bilayer thickness along with adhesion as the

(25) Sneddon, I. N. *Int. J. Eng. Sci.* **1965**, *3*, 47.

Scheme 3. Program Flow Depicting (a) Data Import and Intermediate Calculations, Smoothing, and Initial Threshold Calculation; (b) Data Parsing with Filter, Critical Point Searching, and Extraction and Calculation of Physical Parameters; and (c) Data Output: Force Maps, the Set of Force Curves, Histogram, and Scatter Plots

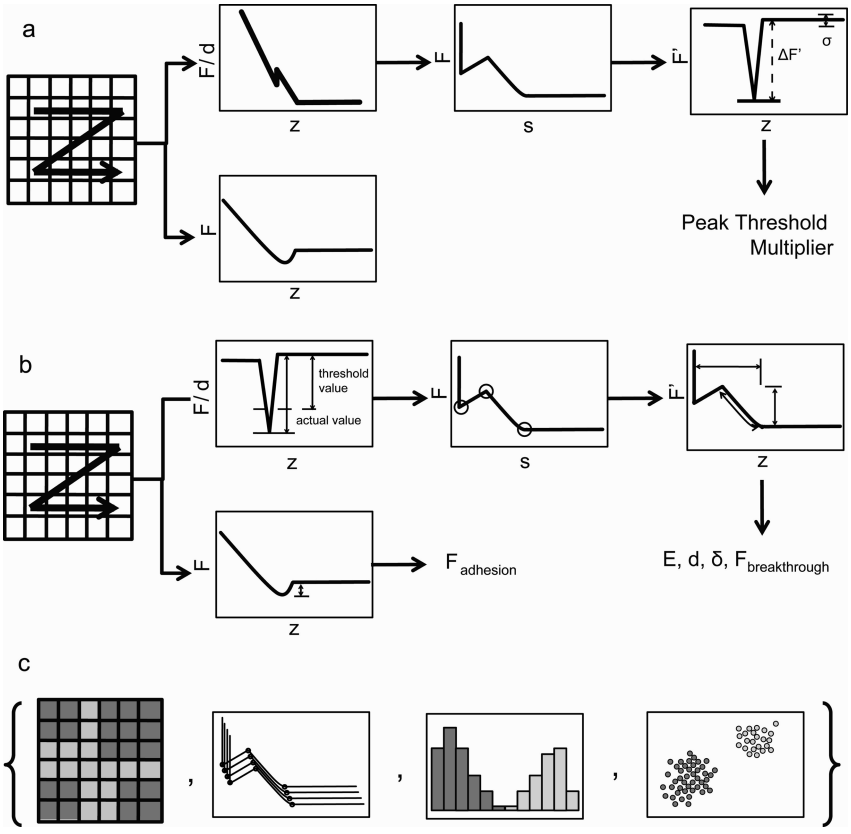

z-scale were created to ascertain any correlation of clusters of data with the spatial distribution of the phases of the lipid bilayer.

Second, the obtained values can also be analyzed statistically, since they represent many repetitions (albeit spatially separated) of tip-indentation experiments. Histograms and scatter plots reveal modalities and correlations in the data, respectively. Figure 2 shows representative output showing both types, as generated by the following analysis procedure: an AFM height image (a) and the corresponding force map of breakthrough forces (b) and Young's modulus values (c), an individual force curve (d), a histogram (e), and a scatter plot for a pair of parameters (f).

In the process of building up this force curve analysis tool, we have created a comprehensive package that facilitates AFM investigation of supported lipid membranes. Recently this automated process has been successfully utilized in elucidating the structure−mechanical property correlation of multicomponent lipid bilayers.[16−18,20] By examining the intrinsic breakthrough forces in bilayers composed of DEC, insight into the organization of the different phases was elucidated. Furthermore, comparison of mechanical properties on DEC with addition of ceramide demonstrated the latter's effect on organization by displacing cholesterol in creating ceramide-enriched domains.[18] Quantifying the mechanical stability of ceramide-enriched lipid bilayers was the objective of a follow-up study, also utilizing this analysis tool.[17] A third study looks at the effects of cholesterol by looking at force maps of a series of lipid membranes with systematic variation of cholesterol content. Furthermore, the effect of tip loading rate on rupture kinetics and activation energies was investigated by again varying velocity values.[16] The variation of two parameters forms a matrix of experiment conditions, and necessitated the collection and analysis of over 30 force maps. The utilization of an automated analysis procedure facilitated this process primarily by ensuring it was accomplished within a realistic time frame.

Force maps have an advantage of direct correlation of topography (morphology) to mechanical properties, which is the reason this AFM technique is important to membrane research. However, due to lengthy manual analysis, one often had to compromise by reducing the resolution of the force map to lower analysis time. Extracting contact point, breakthrough force, and indentation region, and subsequently utilizing them in a series of calculations (elastic modulus, breakthrough force, adhesion force, bilayer thickness), would have made the manual route very tedious, and was the original motivation for designing the program. Table 1 is a comparison of the analysis times of three force volume maps with nearly identical collection parameters. The primary difference between the three force maps is the tip velocity used, which effectively determined the number of points collected per force curve since collection frequency was fixed and force curve distance was set to ∼100 nm. The data sets were analyzed on a midend desktop computer (2.8 GHz Intel Core 2 Quad processor computer with 4GB RAM) and, as the table shows, took between 1 and 6 h to finish, depending on the force curve data point density. At the slowest time and with 4096 curves, this translates to approximately 5 s per force curve, even in light of the fact that the data was largely serially processed and no parallel processing algorithms were explicitly utilized. The software, IGOR Pro, does have a number of built-in, parallel-optimization routines in its curve-fitting functions for multicore processors. However, their effect may be minimal as these were only applied during the elastic modulus calculation step, which consistently took less than 3 min for each of the three data sets—a very small fraction of the total processing time. Because the three data sets exhibited the

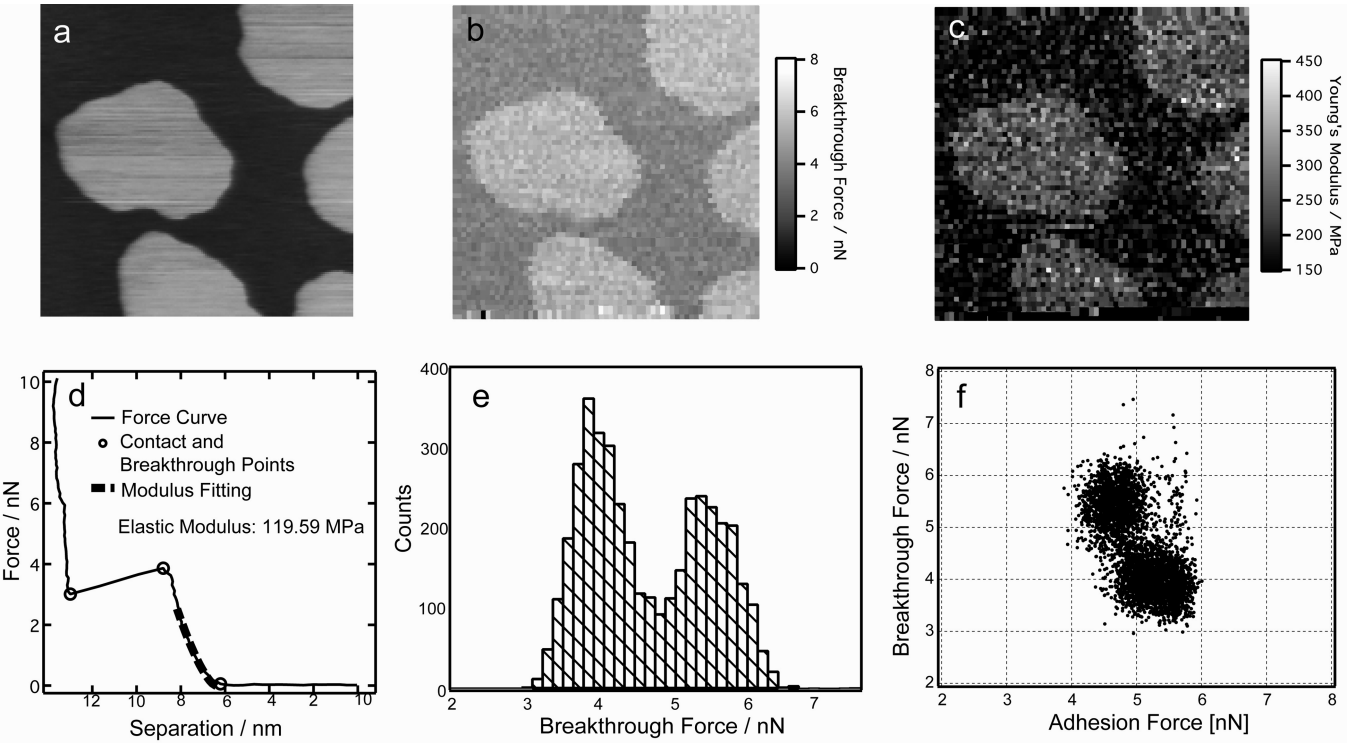

Figure 2. A set of data output: (a) AFM height image (3 μm × 3 μm, z-scale: 0−4 nm from dark to bright); the corresponding recreated force maps of (b) breakthrough forces and (c) Young's Modulus values; (d) representative graph depicting force curve (line), contact and breakthrough points (hollow circles), and curve fit to the Sneddon model (thick dashed line); (e) histogram of corresponding breakthrough forces from panel b; (f) scatter plot showing correlation of breakthrough and adhesion forces.

Table 1. Data Analysis Run Times for Three Force Maps with Very Similar Data Collection Parameters, except for Data Points Per Force Curve

Force Map Parameters			
number of force curves	4096	4096	4096
collection frequency	10 kHz	10 kHz	10 kHz
force distance	∼100 nm	∼100 nm	∼100 nm
tip velocity	2000 nm/s	800 nm/s	200 nm/s
points per force curve	∼1000 points	∼2500 points	∼10000 points
total collection time	**∼25 min**	**∼45 min**	**∼60 min**
Data Analysis Results			
loading time	51 min	51 min	70 min
parsing time	16 min	48 min	289 min
modulus fitting time	2 min	3 min	2 min
total data analysis time	**69 min**	**102 min**	**361 min**

same fitting times, the curve-fitting portion seems to be dependent only on the size of the data set (4096) and not on data point density.

A second advantage is in the use of an automated contact point finder. This part of the software is very crucial, as many subsequent calculations rely on the correct location of the contact point reference. Manual determination of the contact point is usually performed by visual inspection, and is a source of reading error and inconsistency.[26,27] In this program, the location of contact point is quantified by evaluating mean square error of candidate points, with allowance for manual correction if needed.

In designing the code, we also understood that not all force curves were relevant, and had to allow for rejection of some data. One feature that allows adjustment of data acceptance is the average threshold multiplier used in finding the breakthrough force peak in the first derivative of the force curve. This value is calculated per force map and attempts to minimize false positive peaks from significant signal noise, and also missed peaks due to gradual breakthroughs (i.e., nonsharp ruptures). The latter cases would have been viewed as regions that are too stiff to be ruptured, which is not necessarily the correct conclusion if the breakthroughs were just missed. The adjustment of the average threshold multiplier and other factors however, is somewhat empirical in nature because some physics is circumvented with mathematics, and vice versa. For example, the physical dimensions of the system (e.g., the bilayer cannot be more than several nanometers from the substrate, therefore a search algorithm need not traverse coordinates of the force curve farther from the contact point) is used in tandem with searching for function discontinuities to identify breakthrough points.

In the scope of supported lipid membrane experiments, the code lends itself well to utilization of different physical or mathematical models to explain the mechanics. Therefore, its adaptation to other systems (e.g., other thin films, membranes, surfactants), which require force−curve indentation analysis, is straightforward. Moreover, the use of the peak-finding algorithm is also extensible to pulling experiments such as single-molecule pulling studies,[28−31] where, in the case of AFM experiments, it is the retract portion of the force curve that reveals the physics. There has been some work already in the creation of automated algorithms for

(26) Crick, S. L.; Yin, F. C. P. *Biomech. Model. Mechanobiol.* **2007**, *6*, 199.
(27) Sun, Y. J.; Akhremitchev, B.; Walker, G. C. *Langmuir* **2004**, *20*, 5837.
(28) Kellermayer, M. S. Z.; Smith, S. B.; Granzier, H. L.; Bustamante, C. *Science* **1997**, *276*, 1112.
(29) Marszalek, P. E.; Lu, H.; Li, H. B.; Carrion-Vazquez, M.; Oberhauser, A. F.; Schulten, K.; Fernandez, J. M. *Nature* **1999**, *402*, 100.
(30) Rief, M.; Gautel, M.; Oesterhelt, F.; Fernandez, J. M.; Gaub, H. E. *Science* **1997**, *276*, 1109.
(31) Smith, S. B.; Finzi, L.; Bustamante, C. *Science* **1992**, *258*, 1122.

the analysis of single-molecule pulling[32] and receptor−ligand binding experiments.[33,34]

Conclusions

The creation of an automated procedure in the study of lipid membrane systems was motivated by the rich information available from AFM force curves and force maps, whose extraction required a lengthy and tedious process if performed manually. The automated process was able to reduce the total force map processing time, due to heavy reliance on computing power to perform unattended sequential analysis. This therefore enabled the execution of force map experiments requiring a large number of permutations of experimental conditions. The resulting program was successfully used to analyze the indentation and subsequent rupture of supported lipid membranes via AFM tip to extract relevant information that was used to demonstrate structure and mechanics correlation in these systems.

Acknowledgment. This work was supported by the National Research Council (NRC) of Canada Nanometrology program and the National Sciences and Engineering Research Council (NSERC) of Canada Strategic Network (BiopSys, UofT Fund 486163).

(32) Marsico, A.; Labudde, D.; Sapra, T.; Muller, D. J.; Schroeder, M. *Bioinformatics* **2007**, *23*, E231.
(33) Gergely, C.; Senger, B.; Voegel, J. C.; Horber, J. K. H.; Schaaf, P.; Hemmerle, J. *Ultramicroscopy* **2001**, *87*, 67.
(34) Odorico, M.; Teulon, J. M.; Berthoumieu, O.; Chen, S. W. W.; Parot, P.; Pellequer, J. L. *Ultramicroscopy* **2007**, *107*, 887.